Journal of Applied Polymer Science

Bleached extruder chemi-mechanical pulp fiber-PLA composites: Comparison of mechanical, thermal, and rheological properties with those of wood flour-PLA bio-composites

Zhaozhe Yang, Xinhao Feng, Yongbao Bi, Zhifang Zhou, Jinquan Yue, Min Xu
Department of Wood Science and Engineering, Key Laboratory of Bio-based Material Science and Technology (Ministry of Education), College of Material Science and Engineering, Northeast Forestry University, 26 Hexing Road, Harbin 150040, China
Correspondence to: M. Xu (E-mail: xumin1963@126.com)

ABSTRACT: An environmentally friendly bleached extruder chemi-mechanical pulp fiber or wood flour was melt compounded with poly(lactic acid) (PLA) into a biocomposite and hot compression molded. The mechanical, thermal, and rheological properties were determined. The chemical composition, scanning electron microscopy, and Fourier transform infrared spectroscopy results showed that the hemicellulose in the pulp fiber raw material was almost completely removed after the pulp treatment. The mechanical tests indicated that the pulp fiber increased the tensile and flexural moduli and decreased the tensile, flexural, and impact strengths of the biocomposites. However, pulp fiber strongly reinforced the PLA matrix because the mechanical properties of pulp fiber-PLA composites (especially the tensile and flexural strengths) were better than those of wood flour-PLA composites. Differential scanning calorimetry analysis confirmed that both pulp fiber and wood flour accelerated the cold crystallization rate and increased the degree of crystallinity of PLA, and that this effect was greater with 40% pulp fiber. The addition of pulp fiber and wood flour modified the rheological behavior because the composite viscosity increased in the presence of fibers and decreased as the test frequency increased.
 J. Appl. Polym. Sci. **2016**, *133*, 44241.

KEYWORDS: composites; crystallization; fibers; mechanical properties; rheology

Received 21 March 2016; accepted 27 July 2016
DOI: 10.1002/app.44241

INTRODUCTION

Because of their strength and stiffness, natural fibers such as cotton and wood have been used extensively to produce environmentally friendly and sustainable biomaterials to replace gradually diminishing fossil resources such as petro-based materials.[1–4] Biocomposites composed of biodegradable polymers and natural fibers have attracted increasing interest because they can completely degrade in soil without emitting any harmful components and because they present good performance and processing advantages at a favorable cost,[5,6] making them useful in many applications.[7]

Biodegradable polymers produced from renewable resources offer important contributions by reducing the dependence on fossil fuels. They also have positive environmental impacts such as reduced carbon dioxide emissions.[8] Among the commercially available biodegradable thermoplastic polymers, poly(lactic acid) (PLA), made from renewable, natural, resource-derived lactic acid, can be degraded into carbon dioxide, water, and methane over a long period.[9–11] As one of the most promising biodegradable polymers, PLA has attracted extensive investigation as a packaging materials because of its mechanical properties, which are comparable to those of conventional petro-based polymers.[4,6,12] However, PLA has some disadvantages, such as brittleness, low heat resistance, low elongation at break, and a higher price than the frequently used petro-derived polymers polypropylene and polyethylene.[13] These disadvantages have limited its application; therefore, these polymer characteristics must be improved.

Blending PLA with a less expensive filler can reduce the cost of PLA composites and potentially improve their mechanical properties. Natural fibers have been widely used as reinforcement materials for different types of polymer matrices because of their low price, renewability, light weight, abundant natural sources, and total biodegradability.[14] Many investigators have conducted research on reinforcing PLA with different natural fibers such as bamboo,[2,3] flax,[7] kenaf,[10] wood flour (WF),[15] and nanocellulose.[16] Recently, composites composed of PLA and pulp fiber (PF) have been studied extensively.[17–20] Chemical pulp (CP) and thermomechanical pulp were blended with PLA by injection molding, which increased the tensile strength because of the uniform dispersion of the fibers.[17] Higher tensile

Table I. Chemical Composition and Average Dimensions of Wood Flour and Pulp Fiber Raw Material

Fiber	1% NaOH Extractive (%)	Holocellulose (%)	Acid insoluble Lignin (%)	Pentosane (%)	Average length (μm)	Average width (μm)
WF	23.94	75.24	25.14	14.64	293.39	62.42
PF	18.83	80.64	20.54	24.96	302.18	20.84

and impact strengths were attained by adding short and long CP into the PLA matrix than with the neat polymer.[18] High-temperature thermomechanical pulp could slightly improve or retain the tensile and impact strengths when blended with PLA by injection molding.[19] However, the production of all of these different pulps requires energy and water consumption, which leads to some environmental pollution.

Therefore, we selected bleached extruder chemi-mechanical pulp (BECMP) for this study because it has good pulp quality, low consumption of energy and water, low pollution, a short processing sequence, and the availability of relevant commercial equipment.[21] We investigated the influence of the addition this type of PF on the mechanical, thermal, and rheological behaviors of PLA composites prepared by extrusion and hot compression molding. Comparisons of the properties of PLA composites of PF or WF were conducted, and the fractural surface morphologies of the composites were examined using scanning electron microscopy (SEM).

EXPERIMENTAL

Materials

PLA, grade 4032D, was supplied by Nature Works Company (Minnetonka, MN, USA). This polymer has a density of 1.25 g/cm^3, a melt flow index of approximately 30-35 g/10 min (190 °C/2.16 kg) with a glass transition temperature (T_g) and a melting temperature (T_m) of 55–60 °C and 155–160 °C, respectively. WF and PF were produced from poplar wood (*P. adenopoda*) in our laboratory under two different conditions at an average particle size of an 80 mesh screen (Table I). WF was pulverized by a wood fiber pulverizer (Xuzhou Fuyang Energy Science and Technology Corporation, China). PF was manufactured using the BECMP as described in a previous study.[21] All of the raw materials were oven dried at 103 ± 2 °C for 6 h to remove moisture prior to extrusion.

Table II. Formulation of Wood-PLA and Pulp Fiber-PLA Composites

		Weight percent/%	
Specimen	Abbreviation	PLA	Fiber
PLA	PLA	100	0
Wood flour	WF10	90	10
	WF20	80	20
	WF30	70	30
	WF40	60	40
Pulp fiber	PF10	90	10
	PF20	80	20
	PF30	70	30
	PF40	60	40

Composite Processing

Specimens with different proportions (Table II) of WF and PF were weighed and mixed in a high-speed mixer for 10 min and then compounded using a co-rotating twin screw extruder system to produce the WF-PLA and PF-PLA composites. The processing temperature for extrusion was set at 155 °C in the melting zone, 165–175 °C in the pumping zone and 160 °C in the die zone. The rotational speed of the twin-screw was 20 rpm. After extrusion, specimens were compression molded at 185 °C and 15 MPa for 4 min.

Chemical Composition of the Raw Material

The chemical analysis (Table I) of WF and the PF raw material showed 1% NaOH-soluble material, acid-insoluble lignin, pentosane, and hollocellulose in accordance with GB/T2677.5-1993, GB/T2677.8-1994, GB/T2677.9-1994, and GB/T2677.10-1995, respectively.

Fourier Transform Infrared Spectroscopy Analysis

Fourier transform infrared spectroscopy (FTIR) analysis of the WF and PF was performed using a Magna-IR 560 (Thermo Nicolet, USA) at room temperature to determine the difference in the chemical compositions after pulping. Data were collected from 400 to 4000 cm^{-1}, with 32 scans for each specimen. The resolution was 4 cm^{-1}.

Mechanical Testing

Dog-bone tensile specimens (165 × 13 × 4 mm, $L \times T \times R$) were evaluated using a universal mechanical machine (Shenzhen Regear Instrument Cooperation, China) according to ASTM

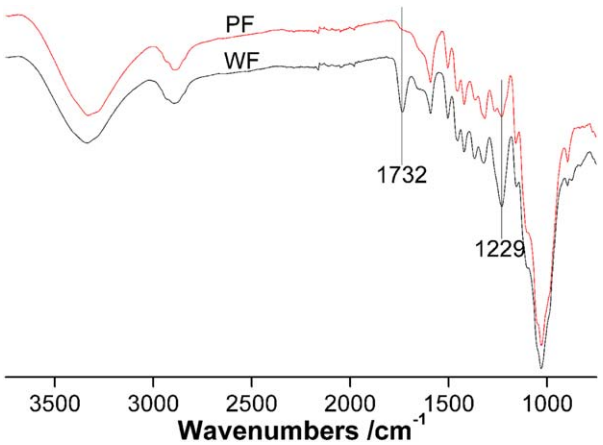

Figure 1. FTIR spectrums of wood flour and pulp fiber. [Color figure can be viewed at wileyonlinelibrary.com.]

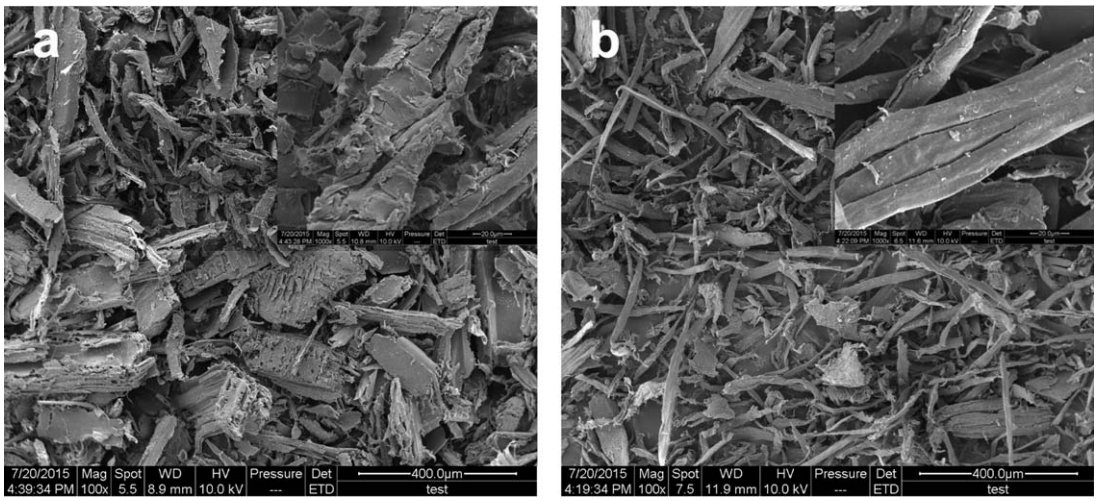

Figure 2. SEM morphologies of wood flour (a) and pulp fiber (b), inserts are surface morphology of a single fiber.

D638-2004. A crosshead speed of 5 mm/min and a gage length of 50 mm were used for the test. Flexural three-point bending specimens (80 × 13 × 4 mm, $L \times T \times R$) were tested using the same universal mechanical machine in accordance with ASTM D790-2004 using a crosshead speed of 1.9 mm/min and a span length of 64 mm. Impact strength specimens (63.5 × 12.7 × 4 mm, $L \times T \times R$) were tested according to ASTM D4812-2004. Six replicates were used for each composite, and the averages with corresponding standard deviations were calculated.

Scanning Electron Microscopy

Both the original and fractured surfaces of the WP-PLA and PF-PLA composite tensile specimens were dried, sputter-coated with gold, and then examined by SEM (FEI QuanTa200 SEM, Holland) at an accelerating voltage of 10 kV.

Differential Scanning Calorimetry

The thermal performances of the products were measured using a TA Q20 (USA) differential scanning calorimeter (DSC). The DSC specimens (approximately 5 mg) were sliced from the composite specimens. The dried specimens were scanned twice at a heating rate of 10 °C/min under a 20 mL/min flow of nitrogen to prevent oxidation. The first scan was to remove all residual moisture and erase any thermal history from 25 to 210 °C, and the specimen was held at 210 °C for 5 min. The samples were then cooled to 25 °C at a rate of 10 °C/min and reheated to 210 °C at a heating rate of 10 °C/min. The endothermic and exothermic peaks obtained from the second scan were termed the glass transition temperature (T_g), the crystallization temperature (T_c), and the melting temperature (T_m). The crystallization enthalpy (ΔH_c) and the heat of fusion (ΔH_m) were also determined from the area of crystallization and the melting peaks, respectively. The cooling and second heating curves were recorded to describe the crystallization and melting behaviors of the nanocomposites. The crystallinity, X_c, was calculated as follows:

$$X_c\ (\%) = 100 \times \left(\Delta H_m / \Delta H_f\ \right) \quad (1)$$

where ΔH_m is the melting enthalpy of the specimen obtained from the second heating curve in the DSC test and ΔH_f is the enthalpy of fusion for the perfectly crystalline PLA (93.6 J/g).[22]

Dynamic Rheological Testing

Dynamic rheological tests were conducted using a rotational rheometer (Discovery HR-2, TA Instruments, New Castle, USA)

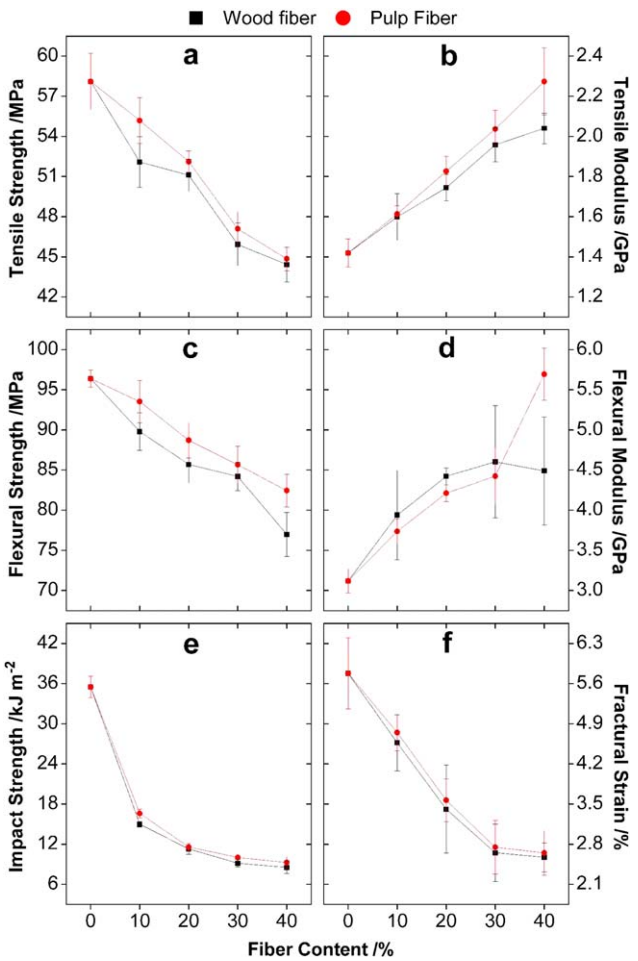

Figure 3. Tensile strength and modulus (a, b), flexural strength and modulus (c, d), impact strength (e), and fractural strain (f) of wood flour-PLA and pulp fiber-PLA composites at different fiber contents. [Color figure can be viewed at wileyonlinelibrary.com.]

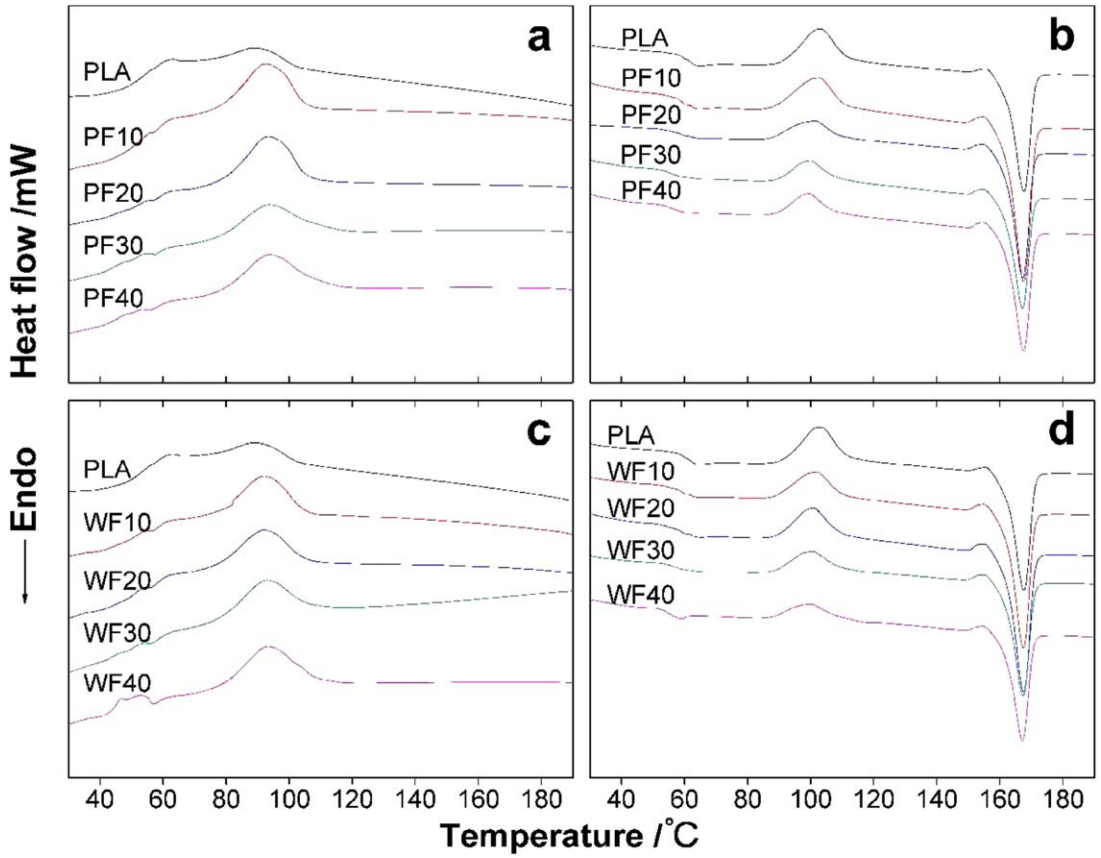

Figure 4. DSC cooling (a,c) and heating (b,d) thermograms for wood flour-PLA (c,d), and pulp fiber-PLA (a,b) composite. [Color figure can be viewed at wileyonlinelibrary.com.]

equipped with a pair of parallel plates (a 2 mm separating distance and 25 mm in diameter). The compression molded specimens were 25 mm in diameter and had a thickness of 2 mm. Prior to testing, the molten specimen was equilibrated for 5 min at 175 °C to erase any previous thermal and deformational history. A dynamic strain sweep was performed first to determine the linear viscoelastic region and then a dynamic time sweep was conducted at an angular frequency of 6.283 rad/s and a strain of 0.01% for 3000 s to ensure that the long-term rheological tests remained in the linear range. A dynamic frequency sweep (0.06–628.3 rad/s) was conducted at a 0.01% strain amplitude in the linear viscoelastic region at 190 °C. Three replicates were evaluated for each formulation.

RESULTS AND DISCUSSION

Chemical Compositions and Morphologies of WF and PF

The chemical compositions of WF and the PF raw materials are shown in Table I. The 1% NaOH-soluble material and acid-insoluble lignin of the WF were 5% higher than those of the PF raw material, whereas the holocellulose and pentosane were 5% and 10% lower, respectively. After BECMP treatment, the PF composition changed significantly, as indicated by the FTIR analyses of WF and PF shown in Figure 1. The peak at 1732 cm^{-1} (the stretching vibration of the non-conjugated keto-group, the carbonyl group, and the ester group in hemicellulose) disappeared, and the peak at 1229 cm^{-1} (the stretching vibration of C-O in the hemicellulose) also decreased in intensity.[23] These results suggest that most of the hemicellulose in the PF was removed by the BECMP treatment, as indicated by the WF and PF morphologies in Figure 2. The WF was podgy [Figure 2(a)], while the PF was slender [Figure 2(b)], and their fiber aspect ratios were 4.7 and 14.5 (Table I), respectively. Furthermore, the WF surface was rougher than the PF surface because of the middle lamellar materials (wax, pectin, lignin, and hemicellulose) remaining on the WF surface [Figure 2(a)]. However, after BECMP treatment, most of the substances associated with the cellulose were removed, resulting in the smooth and clear PF surface shown in Figure 2(b).[24,25]

Mechanical Properties of WF-PLA and PF-PLA Composites

The mechanical properties of the composites are presented in Figure 3. Figure 3(a) shows that the tensile strength of both WF and PF composites decreased with the fiber content because of the poor interfacial adhesion between the PLA matrix and the fibers and the uneven dispersion of the fibers in the PLA matrix,[26,27] as demonstrated by the SEM morphology. However, the tensile strengths of the PF composites were higher than those of the WF composites, especially at 10% fiber content. This is probably because of the higher aspect ratio of PF (as noted previously) and the relatively higher crystallinity of the PF composites, as shown in thermal properties section.[20] The mechanical performance of composites normally depends on

Table III. Thermal Properties of PLA and Its Composites with Wood Flour and Pulp Fiber

Specimen	T_g (°C)	T_c (°C)	ΔH_c (J/g)	T_m (°C)	ΔH_m (J/g)	X_c (%)
PLA	60.8	103.4	21.6	167.6	46.4	49.5
PF10	60.0	102.8	36.1	167.5	56.5	60.4
PF20	58.0	101.2	36.3	167.3	56.6	60.5
PF30	56.2	100.0	38.7	167.1	61.7	65.9
PF40	56.2	99.7	42.3	167.5	65.6	70.1
WF10	58.8	102.0	32.7	167.4	56.2	60.0
WF20	58.0	101.0	37.7	167.4	56.7	60.6
WF30	58.2	100.6	38.9	167.3	58.9	62.9
WF40	55.3	99.8	46.1	167.1	63.4	67.8

five factors: (1) the interfacial adhesion between the matrix and fibers, which is related to the interface stress transfer efficiency; (2) the fraction of fibers; (3) the aspect ratio of the fibers; (4) the fiber orientation; and (5) the degree of crystallinity of the matrix.[28] Therefore, in this study, the interfacial adhesion between the PLA matrix and the fibers was expected to be the main factor influencing the tensile and flexural strengths of composites and resulted in a similar decrease in these properties with the fiber content [Figure 3(a,c)]. However, when comparing with the results of the previous studies,[17,27] the fiber orientation should also be considered because the orientation of the fibers in compression molding is different than that in injection molding.

Unlike the decreased tensile and flexural strengths, the tensile modulus and flexural modulus values increased linearly with the fiber content up to 40% [Figure 3(b,d)] because of the high stiffness of the fibers and efficient stress transfer across the fiber-matrix interface.[18,27] The tensile modulus values of PF composites were a little higher than those of WF composites, whereas the flexural modulus values were similar when the fiber content was less than 40%. At 40% fiber content, the tensile modulus and flexural modulus values of the PF composites were 64 and 78% higher than those of the PLA matrix but only 41 and 40% higher for the WF composites, respectively. PF after BECMP treatment substantially increased the modulus of PLA composites compared to WF.

PLA is a brittle polymer, and its brittleness even increased with the addition of WF and PF. The impact strength [Figure 3(e)] and fractural strain [Figure 3(f)] of the WF and PF composites decreased with fiber additions of 10 to 40%. A significant decrease of 74 and 55% in impact strength and fractural strain, respectively, in both the WF and PF composites at 40% fiber content suggests that poor interfacial adhesion is a sensitive and important factor for the impact strength of composites and that can result in low impact strength of natural fiber composites.[19,29,30] Therefore, the interfacial treatment will be a major focus of our future work, where the effect of reactive coupling agents on the mechanical properties of PLA composites will be tested.

Thermal Properties of WF-PLA and PF-PLA Composites

The thermal properties of the WF-PLA and PF-PLA composites as determined by DSC, are presented in Figure 4. The thermal

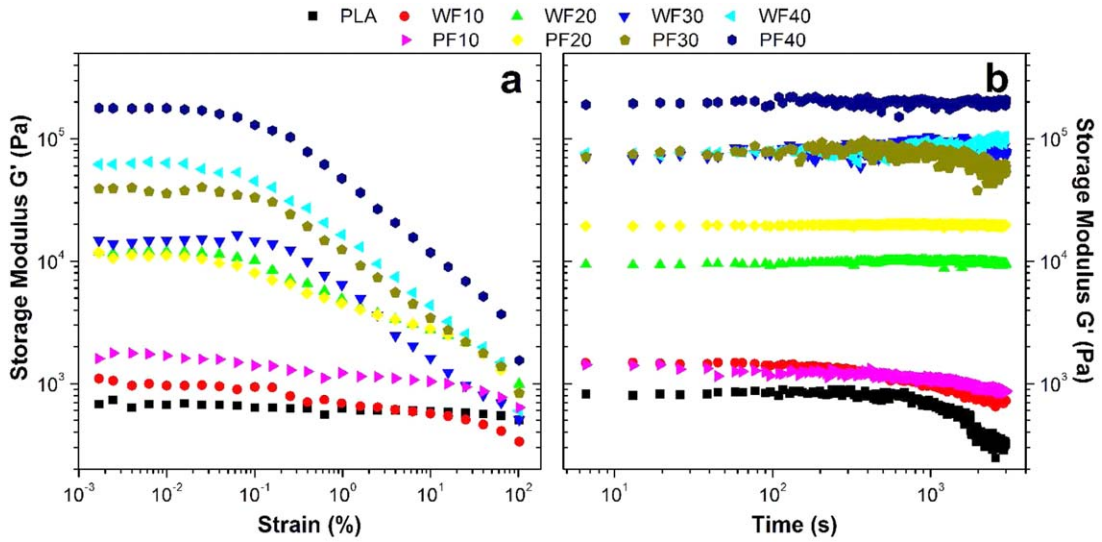

Figure 5. Storage modulus G' of wood flour-PLA and pulp fiber-PLA composites in dynamic strain sweeps at 190 °C, $\omega = 6.283$ rad/s (a) and dynamic time sweeps at 190 °C, $\omega = 6.283$ rad/s and $\gamma = 0.01\%$ (b). [Color figure can be viewed at wileyonlinelibrary.com.]

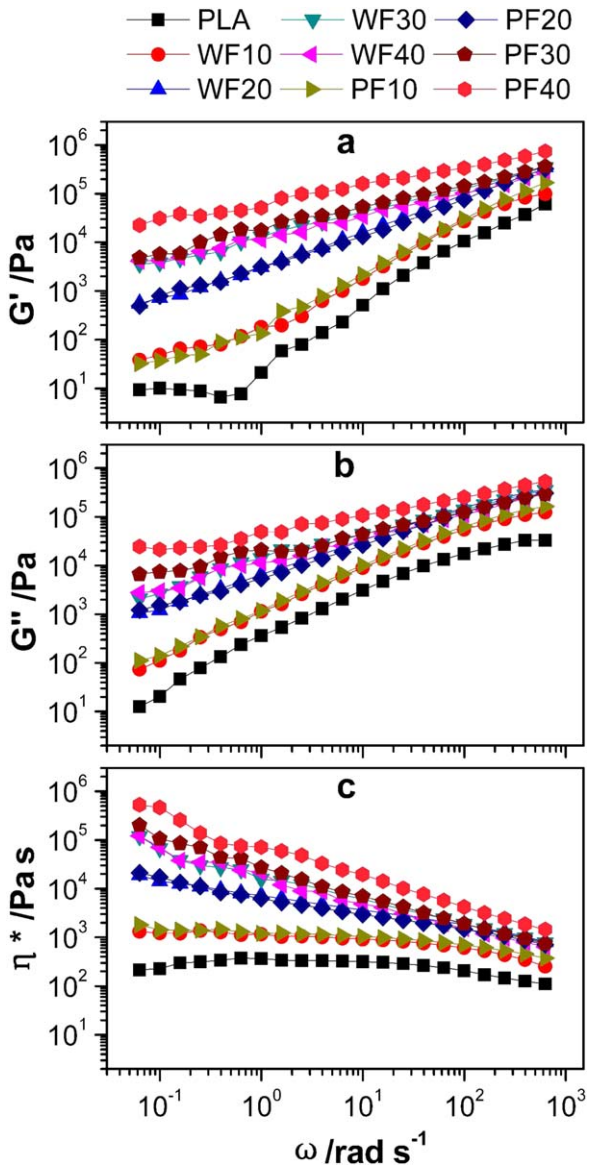

Figure 6. Storage modulus G' (a), loss modulus G'' (b) and complex viscosity η^* (c) of wood flour-PLA and pulp fiber-PLA composites. [Color figure can be viewed at wileyonlinelibrary.com.]

behaviors of the glass transition temperature (T_g), crystallization temperature (T_c), melting temperature (T_m), crystallization enthalpy (ΔH_c), melting enthalpy (ΔH_m), and crystallinity (X_c) obtained from the DSC studies are summarized in Table III. Because of their different relative crystallization rates,[31] PLA showed a small crystallization peak at a cooling rate of 10 °C/min compared with the increased crystallization peaks of the PF and WF composites (after erasing the previous thermal history) as shown in Figure 4(a,c). The melt crystallization temperatures of both PLA and its composites were approximately 95 °C. It appears that WF and PF accelerated the crystallization rate of PLA by acting as a nucleating agent. This was more pronounced in the cold crystallization assessment of the WF-PLA and PF-PLA composites [Figure 4(b,d)]. These results are consistent with other studies on natural fiber/PLA composites,[2,32,33] which reported that natural fibers acted as nucleating agents and improved the crystallization rate when compounded with PLA. Table III shows that the T_c and T_m values of the WF and PF composites did not change significantly with the addition of WF or PF to the PLA matrix. However, the T_g values of both of the WF and PF composites decreased slightly when the fiber content increased from 10% to 40%. This is probably because of the presence of a low fraction of cellulose fibers that contain polar groups (such as hydroxyl groups), and the electrostatic repulsion between these polar groups increased the distance between molecular chains and resulted in a decrease in T_g.[34–36] The crystallinity values (X_c) of the WF and PF composites increased compared to that of the PLA matrix (Table III). This is attributed to the nucleating agent effect of fiber on the PLA matrix. However, the crystallinity of the PF composites was higher than that of the WF composites. The reason may be that the bonding between the PF and the PLA matrix improved because non-cellulosic surface components, such as hemicelluloses and wax, were removed from the fiber surfaces by the BECMP treatment. The increased interaction between the PF and the PLA matrix could further cause the fiber surface to act as nucleation sites for PLA crystallization. Consequently, the PF and PLA composites had increased crystallinity compared to those of composites reinforced with WF.[20,25]

Melt Rheology of WF-PLA and PF-PLA Composites

Dynamic rotational shear measurement is a useful tool to characterize the behavior of a fiber network in a polymer matrix. First, the linear viscoelastic regions of PLA and its composites were determined by a dynamic strain sweep [Figure 5(a)]. The storage modulus, G', of PLA and its composites (10% fiber content) remained linear up to a strain of 10%, and the linear region decreased to 0.1% with increasing fiber content. Therefore, a strain of 0.01% was chosen as the constant for the dynamic time sweeps and the dynamic frequency sweeps of all of the composites. A dynamic time sweep was performed to measure the thermal stability of PLA and its composites at 190 °C, $\omega = 6.283$ rad/s, and $\gamma = 0.01\%$ [Figure (5b)]. The duration of thermal stability of neat PLA at 190 °C was around 800 s. At the same temperature, the addition of fiber increased the stability duration of the composites. For the 40% PF-PLA composites, there was no change in G' even after 3000 s. Because the time required for the dynamic frequency sweep was less than 700 s, the degradation of PLA and its composites could be ignored and did not influence the linear rheological measurements during the rheological test.

The storage modulus, G', and loss modulus, G'', at different loadings for WF-PLA and PF-PLA composites obtained from dynamic rheological measurements are presented in Figure 6(a,b), respectively. Typical homopolymer terminal behavior was expected for PLA, in which the PLA chains would be fully relaxed with the scaling properties of $\sim G' \sim \omega^2$ and $G'' \sim \omega$.[37] The non-terminal behavior of PLA was observed at low frequency, which was attributed to the presence of an ordered domain structure in the polymer system under flow because of the interactions of the molecular chains.[38–40] After fiber additions,

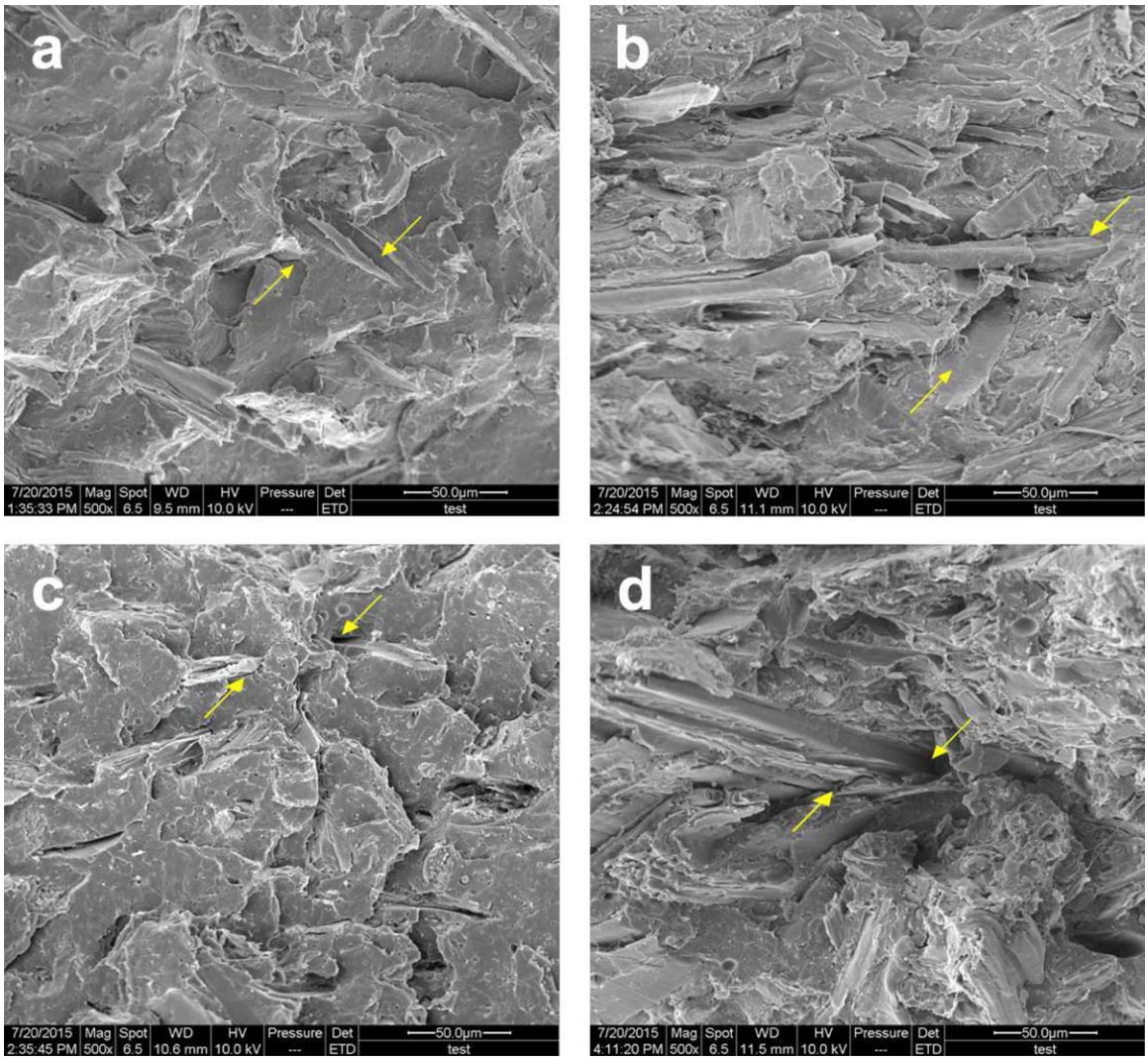

Figure 7. Fractural surface morphologies of 10% (a), 40% (b) pulp fiber-PLA and 10% (c), 40% (d) wood flour-PLA composites. [Color figure can be viewed at wileyonlinelibrary.com.]

the G' and G'' values of the WF-PLA and PF-PLA composites increased with increasing frequency, but the differences between all of the specimens gradually decreased with increasing frequency. The G' and G'' values of the composites also increased with increasing fiber content because of the intrinsic rigidity of the fiber,[38] especially at the highest fiber content. The G' and G'' values of the WF and PF composites overlapped when the fiber contents were below 20%. However, above 30%, the values of the PF composites were higher than those of the WF composites. At 30%, the G' and G'' values of the PF composites were almost same as those of the 40% WF composites, indicating that PF can more efficiently restrict the deformation of the PLA matrix than WF, which was also found for the tensile modulus and the flexural modulus.

Figure 6(c) shows the frequency dependence of the complex viscosity (η^*) for the WF-PLA and PF-PLA composites. The η^* of the PLA showed a Newtonian plateau in the low-frequency range, followed by shear-thinning behavior at higher frequencies. However, in the case of the WF and PF composites, except at 10% fiber content, no Newtonian plateau was observed, and the viscosity continued to increase with decreasing frequency, indicating a pseudo-yield-stress behavior at low frequency. The disappearance of Newtonian behavior at low frequency reveals a transition from liquid-like to solid-like viscoelastic behavior, indicating that the addition of fibers modifies the rheological behavior of the PLA composites because the presence of fibers perturbs the normal polymer flow and hinders the mobility of the chain segments in the flow.[41] At 30% fiber content, the η^* value of the PF composites was slightly higher than that of the WF composites at 40% fiber content at low frequency and nearly same at higher frequency, suggesting that the addition of PF significantly increased the viscosity of composites, which can be explained by both heterogeneous dispersion and the alignment of the fibers in PF composites because of their higher aspect ratio.[38] Therefore, a higher fiber content would further decrease the dispersion of fibers in the melt matrix and result in high-viscosity composites.

Fractural Surface Morphologies of WF-PLA and PF-PLA Composites

The SEM micrographs of the fractural surface of the PF-PLA and WF-PLA composites containing 10 and 40% fiber are presented in Figure 7. At 10% fiber content, it was difficult to distinguish the PF from the PLA matrix because PF was coated by PLA, and torn fibers were found on the surface, was probably because of entangled PF being ripped from the PLA matrix under high loading [Figure 7(a)]. However, holes can be observed on the surface of the WF composites, which are the result of fiber pullout, and gaps are presented between the WF and the PLA matrix [Figure 7(b)], indicating the poor WF-PLA interfacial adhesion. With an increase in fiber content to 40%, a high degree of heterogeneity at the fractural surface of the PF and WF composites was observed along with more torn fibers [Figure 7(b)] and more holes and gaps were found in the matrix [Figure 7(d)], indicating weaker interfacial adhesion in both composites. Figure 2 shows a difference in the surface roughness between PF and WF; a previous study showed that, because of the roughness of the WF, mechanical interlocking contributed to the improved adhesion between WF and PLA.[20] However, in this study, the interfacial adhesion of the WF composites was weaker than that of the PF composites, probably because the higher aspect ratio of PF dominated the interfacial adhesion and compensated for the relatively lower adhesion between PF and the PLA matrix. The morphologies of specimens produced by screw extrusion, injection molding, and compression molding were compared. Oriented fibers were found in the matrix after screw extrusion and injection molding, which resulted in comparable mechanical properties,[19,27] especially for the composites with high fiber aspect ratios.[20] Additionally, the mechanical properties increased with the addition of a coupling agent.[17,26] However, compared with the screw extrusion and injection molding specimens, the compression molded specimen showed non-oriented and unevenly dispersed fibers [Figure 7], leading to decreased tensile strength, flexural strength, and impact strength [Figure 3]. Therefore, the orientation of fibers in the matrix is important for the mechanical properties of composites and should be considered when choosing the fabrication method. Furthermore, the fiber aspect ratio and coupling agents must also be considered to improve the mechanical properties of the composites.

CONCLUSIONS

This study presents the properties of environmentally friendly biocomposites composed of BECMP and PLA that were prepared by twin-screw extrusion followed by hot compression molding. Comparisons of the mechanical, thermal, and rheological properties of PF- and WF-reinforced PLA composites are presented. The tensile and flexural modulus of both composites were greater than those of neat PLA. However, PF achieved greater improvement than WF because of its higher stiffness and efficient stress transfer across the fiber-matrix interface. DSC analysis demonstrated the increase in crystallinity of composites due to the nucleating-agent effect of fibers and suggested that this effect was greater in the PF-reinforced composites. According to dynamic rheometer testing, PF-reinforced PLA composites obtained a higher dynamic viscosity, storage modulus, and loss modulus than WF-reinforced PLA composites at high fiber contents (30 and 40%). This can be explained by both heterogeneous dispersion and the alignment of PF in composites due to their higher aspect ratio. These findings confirmed that PF can be a more efficient reinforcement than WF in PLA matrices. However, the interfacial adhesion of PF and the PLA matrix must still be improved to obtain high mechanical properties. This will be the subject of our future research.

ACKNOWLEDGMENTS

Financial support from the Fundamental Research Funds for the Central Universities (grant number 2572015AB23) is gratefully acknowledged.

REFERENCES

1. Sudesh, K.; Iwata, T. *Clean* **2008**, *36*, 433.
2. Rawi, N. F. M.; Jayaraman, K.; Bhattacharyya, D. *Polym. Compos.* **2014**, *35*, 1888.
3. Yu, Y.; Huang, X.; Yu, W. *Compos. Part B* **2014**, *56*, 48.
4. Orue, A.; Jauregi, A.; Peña-Rodriguez, C.; Labidi, J.; Eceiza, A.; Arbelaiz, A. *Compos. Part B* **2015**, *73*, 132.
5. Bledzki, A.; Gassan, J. *Prog. Polym. Sci.* **1999**, *24*, 221.
6. Saheb, D. N.; Jog, J. *Adv. Polym. Technol.* **1999**, *18*, 351.
7. Oksman, K.; Skrifvars, M.; Selin, J. F. *Compos. Sci. Technol.* **2003**, *63*, 1317.
8. Babu, R. P.; O'Connor, K.; Seeram, R. *Prog. Biomater.* **2013**, *2*, 1.
9. Yang, R. *J. Wuhan. Univ. Technol.* **2015**, *30*, 429.
10. Avella, M.; Bogoeva-Gaceva, G.; Bužarovska, A.; Errico, M. E.; Gentile, G.; Grozdanov, A. *J. Appl. Polym. Sci.* **2008**, *108*, 3542.
11. Zhang, N.; Wang, Q.; Ren, J.; Wang, L. *J. Mater. Sci.* **2009**, *44*, 250.
12. Nampoothiri, K. M.; Nair, N. R.; John, R. P. *Bioresour. Technol.* **2010**, *101*, 8493.
13. Garlotta, D. *J. Polym. Environ.* **2001**, *9*, 63.
14. Xie, Y.; Hill, C. A.; Xiao, Z.; Militz, H.; Mai, C. *Compos. Part A* **2010**, *41*, 806.
15. Teymoorzadeh, H.; Rodrigue, D. *J. Biobased Mater. Bioenergy* **2015**, *9*, 252.
16. Kiziltas, A.; Nazari, B.; Kiziltas, E. E.; Gardner, D. J.; Han, Y.; Rushing, T. S. *Carbohyd. Polym.* **2016**, *140*, 393.
17. Peltola, H.; Pääkkönen, E.; Jetsu, P.; Heinemann, S. *Compos. Part A* **2014**, *61*, 13.
18. Ren, H.; Zhang, Y.; Zhai, H.; Chen, J. *Cell Chem. Technol.* **2014**, *49*, 641.
19. Solala, I.; Koistinen, A.; Siljander, S.; Vuorinen, J.; Vuorinen, T. *BioResources* **2015**, *11*, 1125.
20. Mathew, A. P.; Oksman, K.; Sain, M. *J. Appl. Polym. Sci.* **2005**, *97*, 2014.

21. Yue, J. Q.; Huang, X. L.; Wang, H. Y.; Lu, W. In International Conference of Environment Materials and Environment Management, Harbin, P R China, Du, Z. Y., Sun, X. B., Ed.; Trans Tech Publications LTD: Stafa, Zurich, July 24–25, **2010**.
22. Huang, J. W.; Chang Hung, Y.; Wen, Y. L.; Kang, C. C.; Yeh, M. Y. *J. Appl. Polym. Sci.* **2009**, *112*, 3149.
23. Schwanninger, M.; Rodrigues, J.; Pereira, H.; Hinterstoisser, B. *Vib. Spectrosc.* **2004**, *36*, 23.
24. Shao, Z.; Li, K. *J. Wood Chem. Technol.* **2006**, *26*, 231.
25. Zhang, H.; Ming, R.; Yang, G.; Li, Y.; Li, Q.; Shao, H. *Polym. Eng. Sci.* **2015**, *55*, 2553.
26. Petinakis, E.; Yu, L.; Edward, G.; Dean, K.; Liu, H.; Scully, A. D. *J. Polym. Environ.* **2009**, *17*, 83.
27. Huda, M.; Drzal, L.; Misra, M.; Mohanty, A. *J. Appl. Polym. Sci.* **2006**, *102*, 4856.
28. Dufresne, A.; Dupeyre, D.; Paillet, M. *J. Appl. Polym. Sci.* **2003**, *87*, 1302.
29. Li, H.; Sain, M. M. *Polym. Plast. Technol. Eng.* **2003**, *42*, 853.
30. Colom, X.; Carrasco, F.; Pages, P.; Canavate, J. *Compos. Sci. Technol.* **2003**, *63*, 161.
31. Li, H.; Huneault, M. A. *Polymer* **2007**, *48*, 6855.
32. Masirek, R.; Kulinski, Z.; Chionna, D.; Piorkowska, E.; Pracella, M. *J. Appl. Polym. Sci.* **2007**, *105*, 255.
33. Johari, A. P.; Kurmvanshi, S.; Mohanty, S.; Nayak, S. *Int. J. Biol. Macromol.* **2016**, *84*, 329.
34. Arimura, H.; Ohya, Y.; Ouchi, T. *Biomacromolecules* **2005**, *6*, 720.
35. Gopalan Nair, K.; Dufresne, A.; Gandini, A.; Belgacem, M. N. *Biomacromolecules* **2003**, *4*, 1835.
36. Panagopoulou, A.; Molina, J. V.; Kyritsis, A.; Pradas, M. M.; Lluch, A. V.; Ferrer, G. G.; Pissis, P. *Food Biophys.* **2013**, *8*, 192.
37. Wu, F.; Lan, X.; Ji, D.; Liu, Z.; Yang, W.; Yang, M. *J. Appl. Polym. Sci.* **2013**, *129*, 3019.
38. Shumigin, D.; Tarasova, E.; Krumme, A.; Meier, P. *Mater. Sci.* **2011**, *17*, 32.
39. Lim, Y. T.; Park, O. O. *Macromol. Rapid Commun.* **2000**, *21*, 231.
40. Bhattacharya, S.; Gupta, R. K. In Polymer Nanocomposites Handbook; Gupta, R. K.; Kennel, E.; Kim, K. J., Eds.; CRC press: Boca Raton, **2009**; Chapter 8, p 164.
41. Fortunati, E.; Puglia, D.; Kenny, J. M.; Haque, M. M. U.; Pracella, M. *Polym. Degrad. Stab.* **2013**, *98*, 2742.